Exact enumeration of Hamiltonian circuits, walks, and chains in two and three dimensions

Jesper Jacobsen

Exact enumeration of Hamiltonian circuits, walks, and chains in two and three dimensions

Jesper Lykke Jacobsen[1,2]

[1] LPTMS, Université Paris-Sud, Bâtiment 100,
Orsay, 91405, France
[2] Service de Physique Théorique, CEA Saclay,
Gif Sur Yvette, 91191, France

September 14, 2007

Abstract

We present an algorithm for enumerating exactly the number of Hamiltonian chains on regular lattices in low dimensions. By definition, these are sets of k disjoint paths whose union visits each lattice vertex exactly once. The well-known Hamiltonian circuits and walks appear as the special cases $k = 0$ and $k = 1$ respectively. In two dimensions, we enumerate chains on $L \times L$ square lattices up to $L = 12$, walks up to $L = 17$, and circuits up to $L = 20$. Some results for three dimensions are also given. Using our data we extract several quantities of physical interest.

1 Introduction

The subject of Hamiltonian circuits and walks plays an important role in mathematics and physics alike. Given a connected undirected graph G, a *Hamiltonian circuit* (or cycle) is a cycle (i.e., a closed loop) through G that visits each of the V vertices of G exactly once [1]. In particular, a Hamiltonian circuit has length V. Similarly, a *Hamiltonian walk* (or path) is an open non-empty path (i.e., with two distinct extremities) of length $V - 1$ that visits each vertex exactly once. Note that a Hamiltonian circuit can be turned into a Hamiltonian walk by removing any one of its edges, whereas a Hamiltonian walk can be extended into a Hamiltonian circuit only if its end points are adjacent in G.

We add now to this list of well-known definitions the set $\mathcal{C}_k$ of *Hamiltonian chains* of order k. Each member in $\mathcal{C}_k$ is a set of k disjoint paths whose union visits each vertex of G exactly once (see Fig. 1). The set of Hamiltonian walks is then $\mathcal{C}_1$, and by convention we shall let $\mathcal{C}_0$ denote the set of Hamiltonian circuits. Note that if V is even, $\mathcal{C}_{V/2}$ is the set of dimer coverings of G. The Hamiltonian chain problem has been studied earlier by Duplantier and David on the Manhattan lattice [2], but never to our knowledge on an undirected lattice.

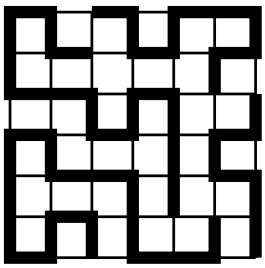

Figure 1: Hamiltonian chain of order 4 on a square lattice of size 7×7.

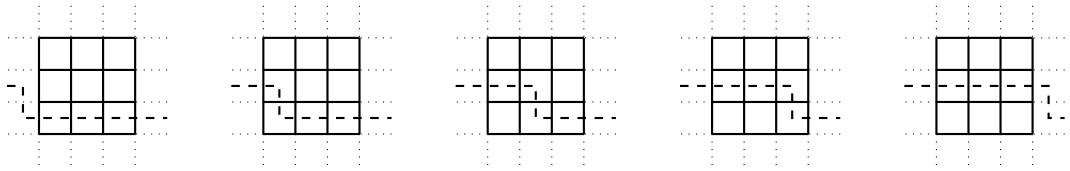

Figure 2: Transfer process for $d = 2$. The lattice is shown in solid line style, with the dotted lines representing lattice edges beyond the bounds of the lattice. The surface $\mathcal{S}$ is shown as a dashed line.

Determining whether G contains a Hamiltonian circuit is a difficult (NP-complete) problem. An even more difficult problem is to determine *how many* distinct Hamiltonian circuits are contained in G. In this paper we shall present an algorithm that efficiently enumerates Hamiltonian circuits, walks, and chains for regular low-dimensional graphs.

The motivation for studying such Hamiltonian structures is by no means limited to graph theory. Indeed, under appropriate solvent conditions, biopolymers such as proteins may fold to form compact conformations, the study of which is currently at the centre of an intense activity in the biophysics community. While real biopolymers contain complicated interactions which can probably not be fully accounted for within any simple lattice model, the study of Hamiltonian walks has been advocated as a first approximation for understanding qualitatively the excluded-volume mechanisms at work behind such problems as polymer melting [3] and protein folding [4]. Our extension to Hamiltonian chains permits to study polydisperse models of several polymers.

Another interest stems from the study of magnetic systems with O(n) symmetry in physics. These can modelled on the lattice as self-avoiding loops (each having the weight n) [5], which, in the limit of vanishing temperature T, are constrained to visit all the vertices [6]. Coupling such systems to a magnetic field H amounts, in a perturbative expansion around $H = 0$, to inserting pairs of loop end points [7]. In the limit $n \to 0$, the partition function Z of the O(n) model at $T = 0$ in a weak magnetic field H can thus be expressed in terms of the number of Hamiltonian chains as

$$Z = \sum_k \mathcal{C}_k H^{2k} \,. \tag{1.1}$$

Finally, the exact enumeration of configurations is useful for settling issues of ergodicity when developing algorithms that provide unbiased sampling of Hamiltonian walks in two [8] and three [9] dimensions.

In section 2 we present our enumeration algorithm and discuss some aspects of its implementation. Results in dimensions $d = 2$ and $d = 3$ are given in section 3. For convenience, we limit the discussion to the simplest lattices (square and cubic), although the construction extends straightforwardly to any regular lattice. Our results are strongest in $d = 2$ where we determine all $\mathcal{C}_k$ for $L \times L$ square lattices up to $L = 12$, $\mathcal{C}_1$ up to $L = 17$, and $\mathcal{C}_0$ up to $L = 20$. In $d = 3$ the largest lattice that we were able to access has size $3 \times 4 \times 4$. Finally, we show in section 4 how to extract physically interesting quantities from our data.

2 Algorithm

We first present our algorithm in dimension $d = 2$ and then discuss the necessary modifications for $d = 3$. For convenience, we limit the presentation to the simplest lattices, viz. an $L_1 \times L_2$ square lattice and an $L_1 \times L_2 \times L_3$ cubic lattice, although the construction extends straightforwardly to any regular lattice. The boundary conditions are free (non-periodic), although it will be clear that it is easy to introduce periodic boundary conditions along *one* of the lattice directions.

The algorithm is based on the transfer matrix principle, according to which the lattice is cut into two parts by means of a conveniently chosen $d - 1$ dimensional oriented surface $\mathcal{S}$. The part of the lattice above (resp. below) $\mathcal{S}$ is called the future (resp. the past). The surface $\mathcal{S}$ cuts the lattice only at mid points of edges.

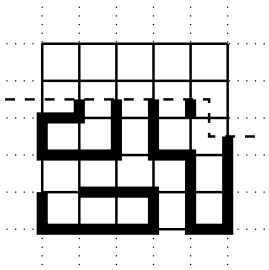

Figure 3: Configuration on a partially constructed 6×6 square.

At the initial (resp. final) step of the enumeration the whole lattice belongs to the future (resp. past), so the algorithm consists in sweeping $\mathcal{S}$ over the entire lattice. This is done by gradually pushing $\mathcal{S}$ towards the future, so that in any one step of the algorithm a *single* vertex is transferred from the future to the past. A few subsequent steps for a 4×4 lattice are shown in Fig. 2.

In any step, the configuration of the system is described by some information about the edges cut by $\mathcal{S}$, and by the number k of chains which have already been completed. The information refered to is the connectivity of the cut edges with respect to the part of the lattice which belongs to the past, and is best illustrated by an example (see Fig. 3). The complete description of the configuration reads in this case $(0, 1, 1, 2, 3, 2|0|1)$, where the first L_1 entries refer to the state of the cut edges which are parallel to the 2-direction (vertical), and the next entry refers to the state of the one cut edge which is parallel to the 1-direction (horizontal). The last entry is the number $k = 1$ of completed chains. In the connectivity part of the information, we use the following coding:

1. A zero entry means an empty edge.

2. Two equal positive entries mean a pair of edges which are connected in the past by part of a chain. Each of these edges will eventually have to be linked to a chain end point in the future, so as to form a complete chain.

3. An unpaired positive entry means an edge which forms part of a partially completed chain, one end point of which has already been fixed in the past. The edge will eventually be linked to another end point in the future, leading to the formation of a complete chain.

It is important to avoid any redundancy in this connectivity information. A unique coding is obtained by requiring that the positive entries (i.e., unpaired entries, or the leftmost member of a pair of equal entries) be arranged in increasing order $(1, 2, 3, \ldots)$ when reading through the coding from left to right.

In step t of the enumeration, the configurations are transfered from "time" t to time $t + 1$. More precisely, each configuration at time t is examined in turn, and all its descendent configurations at time $t + 1$ are generated by exhausting the possible arrangements of the chain at the vertex which is transfered from the future to the past. The information described above is necessary and sufficient for deducing the connectivity information at time $t+1$ from that at time t. Note that since the transfered vertex is not allowed to be empty, there are four possible arrangements if it accommodates a chain end, and six arrangements if a chain passes though it.

Each configuration generated at time $t + 1$ is inserted in an appropriate date structure—a hash table—which also keeps track of its weight (here an integer). The weight of a descendent configuration is the sum of the weights of all the parent configurations that generated it. Some of the generated descendent configurations are however *rejected* before insertion in the hash table (see below). Once step t has been completed, the hash table storing the configurations at time t is erased, and one can move on to step $t + 1$. In this way, only two hash tables (at times t and $t + 1$) are needed in the entire process.

Note that the choice of data structure is essential for the feasibility and the efficiency of the algorithm. A hash table permits to store the configurations via a key which is obtained by reading its coding as one large integer, modulo a suitably chosen prime. Storing and retrieving configurations can

be done in constant time, i.e., independently of the number of configurations being stored in the hash table.

The hash table also allows to keep track of the weight of each configuration, according to the above rule. Namely, when a descendent configuration is generated with weight w, we first make an attempt of looking it up in the hash table at time $t+1$. If it is not there, it is inserted with weight w. If it is already there, w is added to the weight of configuration already present.

If in the transfer process the two ends of the same chain (coded by two equal positive entries) join up, the resulting configuration is rejected, since this would mean forming a cycle rather than a chain. (We make an exception to this rule when the very last vertex is added, since this permits to enumerate $\mathcal{C}_0$.) If an unpaired positive entry gets left behind in the past it means that a chain has been completed, and so $k \to k+1$.

Denote now a general configuration as $(s_{2,1}, s_{2,2}, \ldots, s_{2,L_1}|s_1|k)$. At step $t=0$, the initial state is $(0,0,\ldots,0|0|0)$ and has weight 1. When a row of the lattice is completed, any configuration with $s_1 \neq 0$ gets rejected. When transfering the i'th vertex of the last row, any configuration with $s_{2,i} \neq 0$ gets rejected. This trick allows us to avoid having to deal with a lot of special cases when a boundary vertex is transfered—and also makes it much easier in practice to implement the algorithm correctly. After step $t = L_1 L_2$ the lattice belongs completely to the past, and all the configurations are of the form $(0,0,\ldots,0|0|k)$. Their respective weights are precisely the $\mathcal{C}_k$ that we wanted to compute.

The maximum lattice size that we can attain is essentially limited by the number of different intermediate configurations generated in the transfer process. This number attains its largest value after transfering the next last vertex in the next last row. In practice we could store at most $\sim 10^8$ configurations.

As usual in enumeration studies, the coefficients $\mathcal{C}_k$ are much larger than the integers which are usually represented by a computer ($\leq 2^{32}$ for an unsigned integer on a 32-bit machine). We therefore repeat the enumeration several times, computing each time the result modulo different coprime integers (2^{32}, $2^{31}-1$, $2^{31}-3$,...), and reconstruct the true result in the end by using the Chinese remainder theorem. Note that the use of modular arithmetics is possible because the weights of configurations are constructed only by successive additions of positive integers.

The counts for systems of size $L_1 \times L_2$ and $L_2 \times L_1$ should of course coincide. Verifying that this is indeed the case is however a very strong check of the algorithm, since permuting L_1 and L_2 (with $L_1 \neq L_2$) leads to a completely different transfer process in terms of the propagation of the surface $\mathcal{S}$. We have performed such checks both for $d=2$ and $d=3$.

We now describe briefly how the algorithm can be adapted to a d-dimensional hypercubic lattice of size $L_1 \times L_2 \times \cdots \times L_d$. The surface $\mathcal{S}$ is pushed though the lattice by means of d nested loops, of which the innermost loop (at nesting level $d-1$) moves $\mathcal{S}$ along the 1-direction, etc., and the outermost loop (at nesting level 0) moves $\mathcal{S}$ along the d-direction. In general the loop at nesting level ℓ moves $\mathcal{S}$ along the $(d-\ell)$-direction.

A configuration is given by $(\{s_d\}|\{s_{d-1}\}|\cdots|\{s_1\}|k)$, where the space $\{s_\ell\}$ describes the edges cut by $\mathcal{S}$ which are parallel to the ℓ-direction and consists of $\prod_{i=1}^{\ell-1} L_i$ entries. When the loop at nesting level $d-\ell$ is executed for the last time, the entry in $\{s_\ell\}$ corresponding to the position of the loops at nesting levels $> d-\ell$ must be zero; otherwise the configuration is rejected.

At each vertex there are $2d$ possible local arrangements if the vertex contains a chain end, and $\binom{2d}{2}$ arrangements if it does not.

We have implemented the algorithm for $d=2$ and $d=3$. It is of course most efficient in low dimensions when the number of entries necessary to describe a configuration is small, and the configurations themselves are strongly constrained by topology. We were however able to obtain useful results as well for $d=3$ (see below).

3 Results

3.1 Two dimensions

We first present our results in two dimensions.

k	$\mathcal{C}_k$
0	1076226888605605706
1	3452664855804347354220
2	4105040900990127258563352
3	1716401559105599779087093260
4	3636520562172171712062430353 40
5	4614804195743592698824499969 2732
6	3870392655399966034741749180958852
7	2290004447978396868052132145954706 48
8	1001402619377724129976669288068603 5774
9	3351266327816347764359816058081533 10160
10	8818298873873444121262995871243309826506
11	1864253364159023843432163894619273301722 68
12	3222564357088784934867009058887596660853042
13	4621682229212699841347628198532439650724 5748
14	5566937877838626089279846983863634701879819 38
15	5690759125611797657956588062161464969526622268
16	4981285533935287526344985139418374399217789 4504
17	3762595235577997904900765630920799573679714 41020
18	2469068810121023544317004188530710352090945411914
19	1415925860385478189236161052852846509087258248 2860
20	7132860684366029309952672381789022614932499605 1770
21	3170979334498024406423042920964632082537520028 53220
22	1249084471204154623059161399602853755323161718519772
23	4375441585007318378166364769735565649135514407725428
24	1367322733070373191369404964395259640576611353410 3766
25	3822704157817778299392672263888324831630323860948 5072
26	9585454312919597088375149975920979843362981114056 0618
27	2160543243152619092731421992358229750415398614781215 08
28	4386042471850123335575300437826009457552075682306435 94
29	8033202611781567397154031636472911258631984702035380 48
30	1329413609161899137884978107235777594261127805779481138
31	1990427307505969944020236847124806666399811554129750496
32	2699118726122396972411170136925985393885382039591724116
33	3318040996252249925481740087801704155429556174343699608
34	3700359327341155923554786919768922871490843218081792948
35	3745875480760985174397430937750746156033853657449987776

Table 1: Number $\mathcal{C}_k$ of Hamiltonian chains of order k (i.e., consisting of precisely k chains) on a 12×12 square lattice.

k	$\mathcal{C}_k$
36	344337050255880729056235400083638573226820848552113903 0
37	28750087893679226598480835222437223633552246827344422 0
38	21804937634756452007736179706786583438788707561017851 54
39	15020953913706715757729871300768646429557252125073975 12
40	93964772481971669338857932911645635013504265027087234 0
41	53356285383915485534192796509721014685170748133226443 6
42	27486264249669929025229099016027905717593035232409182 4
43	12836255539974371943487735257959263089586076479477462 4
44	54294968510865162278386828132399087185256262942414932
45	20778050812329434163278524326813392470106157931284728
46	71847868457846504253127093232601986740849095327762 92
47	22414823410863370658944900749203077558103066933109 36
48	62982381571595313333156048899190401467856209126804 2
49	15907724553440447939332455293162400043846673596602 0
50	36035273248074550220433523348607010222299409542106
51	73025439150288812572993619349450607986792837268 08
52	13200742151069421248736593316925198270580554056 44
53	21217240913663790010662957622956552942562898136
54	30209940418516563152074763182692186029320843454
55	37946682495061005682688766608363835365236538 16
56	41851274723913098628268688584052629104406369 2
57	40310331424536568202368529058344353430213252
58	33699255054748147979462148484248895863369 52
59	24279432704321827924292374405368040974531 6
60	14951909347540490900851120307089218715790
61	77949364740771636380822990073456271135 6
62	34012688096545799769214778699372499928
63	12253433732360441191397093338197225 48
64	35847082988635315875798770248538788
65	83422315118501510474256652743969 6
66	15044012072281443196476714201368
67	20312312995130550254618613649 6
68	19589186107593359965167052 96
69	12602334728369293472453184
70	48539905585658564517760
71	91904378228899701504
72	53060477521960000

Table 1: (continued).

L	$\mathcal{C}_1$
2	4
3	20
4	276
5	4324
6	229348
7	13535280
8	3023313284
9	745416341496
10	730044829512632
11	786671485270308848
12	3452664855804347354220
13	1665200571767053468131558O
14	331809088406733654427925292528
15	726361136796026649026260011725152O
16	662634717384979793238814101377988786884
17	664289947391594699694401195797368076126655O

Table 2: Number $\mathcal{C}_1$ of Hamiltonian walks on an $L \times L$ square lattice, up to size $L = 17$.

L	$\mathcal{C}_0$
2	1
4	6
6	1072
8	4638576
10	467260456608
12	1076226888605605706
14	561264996204914372812636O8
16	6588251652262583632615978616553057O
18	1733926377888966183927790794055670829347983946
20	10204604273907687935430269656781528315710730526624280971O6

Table 3: Number $\mathcal{C}_1$ of Hamiltonian circuits on an $L \times L$ square lattice, up to size $L = 20$.

We have been able to solve the full Hamiltonian chain problem for $L \times L$ square lattices up to size $L = 12$. The number of circuits $\mathcal{C}_0$ vanishes when L is odd by an easy parity argument, but the remaining $\mathcal{C}_k$ with $k = 1, 2, \ldots, \lfloor L^2/2 \rfloor$ are all non-zero. The complete result for $L = 12$ is shown in Table 1.

When L is even, $\mathcal{C}_{L^2/2}$ should be the number $\mathcal{D}_L$ of dimer coverings of an $L \times L$ square lattice. We have checked that our data agree with the analytical results [10] for $\mathcal{D}_L$ for all $L = 2, 4, 6, 8, 10, 12$.

If only the first few $\mathcal{C}_k$ are needed, the enumeration can be taken to larger sizes by rejecting all states $(s_{2,1}, s_{2,2}, \ldots, s_{2,L_1} | s_1 | k)$ with $k > k_{\max}$.

In particular, we have obtained the number $\mathcal{C}_1$ of Hamiltonian walks up to size $L = 17$; see Table 2. This extends the $L \leq 7$ results by Mayer *et al* [11] by ten new terms. Note also that Jaeckel *et al* [12] have proposed a Monte Carlo method for estimating $\mathcal{C}_1$ for larger L. These authors obtain $1.3582 \cdot 10^7$ for $L = 7$—that is 0.3 % above the exact result—and $2.7791 \cdot 10^9$ for $L = 8$—that is 29 % below the exact result.

Variant Hamiltonian walks, constrained to have their end points on diametrically opposite corners of an $L \times L$ square with L even, have been studied in [13]. Since this is technically an easier problem than our unconstrained walks, the enumerations could be taken to size $L = 34$.

Finally, we have obtained the number $\mathcal{C}_0$ of Hamiltonian circuits up to size $L = 20$; see Table 3. This extends the $L \leq 16$ data [14] by two new terms.

k	$2\times2\times2$	$2\times2\times3$	$2\times3\times3$	$3\times3\times3$	$3\times3\times4$
0	6	22	324	0	3918744
1	72	584	16880	2480304	677849536
2	204	4204	270756	104844792	40656040968
3	108	7604	1281376	1246834176	816646740296
4	9	4541	2507084	6520250088	7803954743412
5		852	2281064	17852434656	41553510978656
6		32	985354	27873228036	134709106959932
7			190580	25864316448	280608712776492
8			13834	14445212196	388267754276278
9			229	4798350687	363680422635635
10				911288760	232420898624633
11				91325100	101132591631452
12				4119048	29594655770318
13				57048	5683316575620
14					687432832414
15					48991382300
16					1837669320
17					29304199
18					117805

Table 4: Number $\mathcal{C}_k$ of Hamiltonian chains of order k on various cubic lattices of size $L_1 \times L_2 \times L_3$. Blank entries are zero.

3.2 Three dimensions

Our results for the full Hamiltonian chain problem on small $L_1 \times L_2 \times L_3$ parallelepipeds are given in Table 4. In addition we find for the $3 \times 4 \times 4$ system a number of $\mathcal{C}_0 = 3777388236$ circuits and $\mathcal{C}_1 = 1073054619800$ walks.

Note that the transfer matrix method is essentially limited by the area of the smallest cross section of the parallelepiped. It would thus be possible to extend the enumerations to some systems with, say, $L_1 = L_2 = 3$ and $L_3 \geq 5$, but we have chosen to focus here on close-to-cubic shapes which are the most challenging.

The number of walks $\mathcal{C}_1$ has been much studied in the area of protein research [15, 16], whereas the numbers $\mathcal{C}_k$ with $k \neq 1$ have to our knowledge not been considered previously. Note that the works [15, 16] were based on direct enumeration, meaning that in contrast to our transfer matrix method each individual conformation was actually generated. The limitation of direct enumeration is thus the number of conformations being counted, since the CPU time requirement is (at best) proportional to this. Accordingly, Ref. [16] uses massively parallel supercomputer facilities to access the $3 \times 4 \times 4$ system. By contrast, our transfer matrix approach is limited rather by the memory than the CPU time. Unfortunately, this memory limitation put the $4 \times 4 \times 4$ system just a little outside our reach. On the other hand, the counts for the $3 \times 4 \times 4$ system were made very fast, in just a few minutes.

In Refs. [15, 16] the counts were produced modulo the symmetry group of the lattice. For the $2 \times 2 \times 2$ and the $3 \times 3 \times 3$ systems, our results for $\mathcal{C}_1$ come out as exactly 24 times those of [15]. For the $3 \times 3 \times 4$ and $3 \times 4 \times 4$ systems, our results for $\mathcal{C}_1$ are precisely 8 times those of [16]. This means that for each of these systems, all Hamiltonian walks are unrelated by lattice symmetries.

4 Applications

The enumerations reported above conceal many quantities of physical relevance. We discuss here some of them.

4.1 Conformational exponents

The radius of gyration R of a polymer of length $l \gg 1$ is expected to scale like

$$R \sim l^{\nu} \tag{4.1}$$

where ν is a standard critical exponent [7]. For Hamiltonian walks on an L^d hypercube in d dimensions, we have obviously $R \sim L$ and $l \sim L^d$, and so $\nu = 1/d$. Non-trivial information is however contained in the number of circuits and walks, here both supposed to have one marked monomer attached to a fixed point:

$$\tilde{\mathcal{C}}_1 \sim \mu^l l^{\gamma-1}\,, \qquad \tilde{\mathcal{C}}_0 \sim \mu^l l^{-\nu d}\,. \tag{4.2}$$

Here μ is the so-called connective constant, and γ is another critical exponent [7]. In our setup, the circuits are unmarked and the end points of the walks are free to be anywhere on the lattice, and so

$$\mathcal{C}_1/\mathcal{C}_0 \sim l^{\gamma+1} \sim L^{(\gamma+1)d}\,. \tag{4.3}$$

In addition to this leading behaviour there are subdominant corrections due to surface effects.

In two dimensions, we can extract results for μ and γ using the data in Tables 2–3. Due to parity effects, this is best done by working in terms of the ratios $\frac{\eta(L+2)}{\eta(L)}$, where $\eta(L) = \mathcal{C}_0(L)$ for even L or $\mathcal{C}_1(L)$ for any parity in the case of μ, and $\eta(L) = \mathcal{C}_1(L)/\mathcal{C}_0(L)$ for even L in the case of γ. The naive approximants are further extrapolated using standard finite-size scaling techniques. This gives

$$\begin{aligned} \mu &= 1.473 \pm 0.001\,, \\ \gamma &= 1.042 \pm 0.003\,. \end{aligned} \tag{4.4}$$

Our estimate for μ is in good agreement with (but less accurate than) the currently best known estimate [6]

$$\mu = 1.472801 \pm 0.00001\,. \tag{4.5}$$

Note that the latter uses exact predictions from field theory for the leading finite-size corrections, a scheme that we have not adopted here. The constrained Hamiltonian walks considered in [13] led to a consistent value for μ. The long-standing history of numerical and analytical estimates for μ of Hamiltonian walks can be found in the introductions of [12, 6].

Our estimate for γ is a nice confirmation of the exact field theoretical result [6]

$$\gamma = \frac{117}{112} = 1.04464\cdots \tag{4.6}$$

Previous numerical results, as discussed in [6] and references therein, were obtained in a cylindric geometry and assumed certain results of conformal field theory. The present estimate therefore furnishes a more direct verification of the exact result (4.6).

4.2 Contact probabilities

As already mentioned in the introduction, a Hamiltonian circuit can be turned into a Hamiltonian walk by removing any one of its edges, whereas a Hamiltonian walk can be extended into a Hamiltonian circuit only if its endpoints are adjacent. This implies that the probability that the two end points of a walk are adjacent is

$$p_{\mathrm{adj}} = \frac{\mathcal{C}_0 L^d}{\mathcal{C}_1}\,. \tag{4.7}$$

In two dimensions, the p_{adj} for $L \times L$ square can be computed from Tables 2–3. The resulting numerical values are displayed in Table 5. Note that p_{adj} vanishes for odd L (as it does on any bipartite lattice having an odd number of vertices).

The values in Table 3 have been used in [8] to test that a certain Monte Carlo algorithm for producing Hamiltonian walks did indeed give unbiased results.

L	p_{adj}
2	1.00000000000000000000
4	0.34782608695652173913
6	0.16826830842213579364
8	0.09819321919798768694
10	0.06400435120127304050
12	0.04488610346836087660
14	0.03315398616246303584
16	0.02545282308230371747

Table 5: Probability p_{adj} that the two end points of a Hamiltonian walk on an $L \times L$ square lattice are adjacent.

Physically, on may argue that p_{adj} is proportional to the probability that the two ends of an open polymer (walk) join so as to form a ring polymer (circuit).

It is tempting to try similarly to construct from the ratio of $\mathcal{C}_1$ and $\mathcal{C}_2$ the probability that the conformation of two chains is such that one end point of each are adjacent on the lattice. Unfortunately, this is not possible, since certain two-chains (more precisely those in which an end point of one chain is adjacent to both end points of the other chain) can be obtained from more than one one-chain by removing an internal edge in the latter.

4.3 Lee-Yang zeroes

The study of phase transitions through the location of partition function zeroes in the complex magnetic field plane was initiated by Yang and Lee [17]. In particular, these authors established that for the Ising model these zeroes lie on the unit circle in terms of the variable $x = \mathrm{e}^{2H}$, i.e., they correspond to purely imaginary values of the field H. The zero closest to the positive real axis is denoted $\mathrm{e}^{i\theta_{\mathrm{c}}}$, where θ_{c} is the so-called Lee-Yang edge. At the critical temperature, $\theta_{\mathrm{c}} \to 0$ in the thermodynamic limit, and its finite-size scaling permits to access a critical exponent. Another possible approach is to study the density of zeroes $g(\theta)$. Creswick and Kim [18] have shown that at the critical temperature $g(\theta) \sim |\theta|^{1/\delta}$ for $\theta \ll 1$.

We have studied the zeroes of the partition function (1.1) in terms of the variable $y = -H^2$ for $L \times L$ squares with $L \leq 12$. For odd L there is one trivial zero at $y = 0$ (since $\mathcal{C}_0 = 0$), and for even L the two zeroes closest to $y = 0$ form a complex conjugate pair with an imaginary part that tends to zero as $L \to \infty$. Disregarding these "exceptional" zeroes, all the remaining zeroes (for L of any parity) are found to lie on the positive real axis in the complex y-plane, corresponding to purely imaginary H as in the Lee-Yang theorem.

We now define a finite-L approximation to the density of zeroes in the point y_n as $g(y_n) = \frac{1}{y_{n+1} - y_n}$, where we have arranged the zeroes of $Z(L \times L)$ in increasing order $y_1 < y_2 < \ldots < y_N$.

The approximations $g(y)$ are shown in Fig. 4 for $L = 9, 10, 11, 12$. One observes a clear crossover near $y = 1$, separating two regimes of power law behaviours. For even L the curves bifurcate for $y \ll 1$, which can be remedied by regrouping the zeroes two by two (not shown). The power laws extracted from the largest available sizes read

$$g(y) \sim \begin{cases} y^{-0.46} & \text{for } y \ll 1 \\ y^{-1.66} & \text{for } y \gg 1 \end{cases} \tag{4.8}$$

We have no satisfying explanation for these exponents at present. The naive application of the standard scaling laws $\nu d = 2 - \alpha$ (Josephson) and $\alpha + 2\beta + \gamma = 2$ (Rushbrooke), and the results $\nu = \frac{1}{2}$ and $\gamma = \frac{117}{112}$ for the critical $y = 0$ system [6], leads to $1/\delta = -\frac{5}{229} = -0.0218\cdots$, which is clearly off the mark.

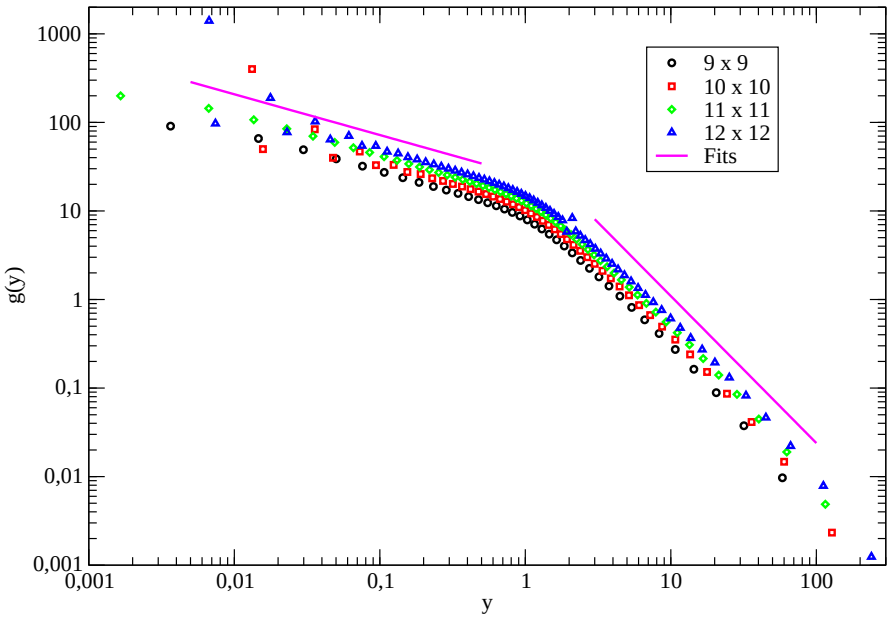

Figure 4: Density $g(y)$ of partition function zeroes in the variable $y = -H^2$ for the Hamiltonian chain problem on $L \times L$ squares.

Acknowledgments

This work was supported through the European Community Network ENRAGE (grant MRTN-CT-2004-005616) and by the Agence Nationale de la Recherche (grant ANR-06-BLAN-0124-03).

References

[1] W.R. Hamilton, Phil. Mag. **12** (1856); Proc. Roy. Irish Acad. **6** (1858).

[2] B. Duplantier and F. David, J. Stat. Phys. **51**, 327 (1988).

[3] P.J. Flory, Proc. Roy. Soc. London A **234**, 60 (1956).

[4] K.A. Dill, Protein Science **8**, 1166 (1999).

[5] B. Nienhuis, Phys. Rev. Lett. **49**, 1062 (1982).

[6] J.L. Jacobsen and J. Kondev, Nucl. Phys. B **532**, 635 (1998).

[7] P.-G. de Gennes, *Scaling concepts in polymer physics* (Cornell University Press, New York, 1979).

[8] R. Oberdorf, A. Ferguson, J.L. Jacobsen and J. Kondev, Phys. Rev. E **74**, 051801 (2006).

[9] J.L. Jacobsen, preprint (2007).

[10] P.W. Kasteleyn, Physica **27**, 1209 (1961).

[11] J.-M. Mayer, C. Guez and J. Dayantis, Phys. Rev. B **42**, 660 (1990).

[12] A. Jaeckel, J. Sturm and J. Dayantis, J. Phys. A **30**, 2345 (1997).

[13] M. Bousquet-Mélou, A.J. Guttmann and I. Jensen, J. Phys. A **38**, 9159 (2005).

[14] Sequence A003763 in N.J.A. Sloane (ed.), *The online encyclopedia of integer sequences*, `http://www.research.att.com/~njas/sequences/`.

[15] E. Shakhnovich and A. Gutin, J. Chem. Phys. **93**, 5967 (1990).

[16] V.S. Pande, A.Y. Grosberg, C. Joerg and T. Tanaka, J. Phys. A **27** 6231 (1994).

[17] C.N. Yang and T.D. Lee, Phys. Rev. **87**, 404 (1952); *ibid.* **87**, 401 (1952).

[18] R.J. Creswick and S.-Y. Kim, Phys. Rev. E **56**, 2418 (1997).